GEOLOGY

Copper isotope evidence for sulfide fractionation and lower crustal foundering in making continental crust

Sheng-Ao Liu[1]*, Roberta L. Rudnick[2], Wen-Ran Liu[1], Fang-Zhen Teng[3], Tian-Hao Wu[1], Ze-Zhou Wang[3]

The continental crust is strongly depleted in copper compared with its building blocks—primary arc magmas—and this depletion is intrinsically associated with continental crust formation. However, the process by which Cu removal occurs remains enigmatic. Here we show, using Cu isotopes, that subduction-zone processes and mantle melting produce limited fractionation of Cu isotopes in arc magmas, and, instead, the heterogeneous Cu isotopic compositions of lower crustal rocks, which negatively correlate with Cu contents, suggest segregation or accumulation of isotopically light sulfides during intracrustal differentiation of arc magmas. This is supported by the extremely light Cu isotopic compositions of lower crustal mafic cumulates and heavy Cu isotopic compositions of differentiated magmas in thick continental arcs. Intracrustal differentiation of mantle-derived magmas and subsequent foundering of sulfide-rich mafic cumulates preferentially removes isotopically light Cu, leaving a Cu-depleted and isotopically heavy continental crust.

INTRODUCTION

The continental crust has a bulk andesitic composition (*1*), which is evolved compared to primary mantle-derived magmas at both convergent margins and within plates that are predominantly basaltic (*2*). Therefore, the bulk continental crust (BCC) cannot be directly derived from partial melting of the mantle (*3*–*5*). The origin of the evolved continental crust is an intriguing and enigmatic problem. The BCC is depleted not only in magnesium but also in copper and other chalcophile elements (e.g., Au and Ag) compared with basaltic arc magmas and mid-ocean ridge basalts (MORBs) (*6*, *7*). It has an average Cu concentration ([Cu]) of ~27 parts per million (ppm) (*1*), less than half that of primitive arc lavas (~60 ppm) and MORB (~80 ppm) (Fig. 1A). Unravelling the origins of the continental crust's Cu deficit will help constrain its formation and evolution and allow for a better understanding of the genesis of porphyry Cu systems. For example, porphyry copper deposits form mainly in continental arcs with thick crust (*8*, *9*), but the reason is not fully understood, given that the continental crust is strongly Cu-depleted.

Arc magmas are the major building blocks of the continental crust (*5*, *10*, *11*), and two hypotheses have been advocated to explain the crust's Cu deficit. On the basis of the systematic difference in Cu content between arc magmas in arcs with thin crust and those in arcs with thick crust, previous studies concluded that Cu is concentrated in the lower crust via intracrustal magmatic differentiation involving sulfides in thick arcs, followed by foundering of the sulfide-bearing mafic/ultramafic cumulates into the mantle, leaving behind a Cu-depleted, evolved continental crust (*6*, *7*, *12*, *13*). However, the Cu systematics of arc magmas depend on multiple factors, including Cu and sulfur contents, oxygen fugacity (fO_2) and degree of melting of the subarc mantle sources (*14*, *15*), in addition to magmatic differentiation. For example, the low Cu contents of magmas erupted in thick arcs might also result from lower-degree melting of a sulfur-rich mantle (*15*). Thus, the origin of the Cu deficit in both evolved arc magmas and the continental crust is uncertain.

This ambiguity regarding the origins of the continental crust's Cu depletion can be addressed by examining Cu isotopes because, unlike [Cu], Cu isotopes are essentially unfractionated during partial melting of the mantle, regardless of the melting degree and the presence of residual sulfide (*16*, *17*), which is Cu-poor monosulfide solid solution and/or sulfide melt (*18*). Various types of basalts formed by different degrees of mantle melting all have mantle-like Cu isotopic compositions (δ^{65}Cu) (Fig. 1B). By contrast, substantial Cu isotope fractionation occurs during magmatic differentiation that involves more Cu-rich sulfides; these sulfides have δ^{65}Cu that is more than 2‰ lower than equilibrium silicate melts at temperatures below ~1100 K (Fig. 1B) (*19*–*22*). Moreover, if redox reactions involving Cu reduction from silicate melt to sulfide occur during sulfide crystallization, then Cu isotope fractionation is more than one order of magnitude larger than in the absence of these reactions (*23*). These properties make Cu isotopes a powerful tool for identifying sulfide fractionation during intracrustal differentiation of mantle-derived magmas, thereby helping to determine the origin of the Cu deficit in the continental crust.

Here, we report [Cu] and δ^{65}Cu in lower crustal rocks, sulfide-rich continental arc cumulates, arc basalts and basaltic andesites erupting through a thick (continental) crust, and a suite of subduction-zone prograde metamorphosed rocks (fig. S1). These samples are used to characterize the Cu isotopic composition of the lower continental crust (LCC), to investigate the behavior of Cu isotopes during intracrustal differentiation of basaltic magmas in thick (continental) arcs, to elucidate the behavior of Cu isotopes during slab dehydration, and to assess the Cu isotopic heterogeneity of arc magma sources. Our results reveal substantial Cu isotope heterogeneity in lower crustal rocks and cumulates, which suggests that intracrustal sulfide fractionation of basaltic magmas and subsequent

[1]State Key Laboratory of Geological Processes and Mineral Resources, China University of Geosciences, Beijing 100083, China. [2]Department of Earth Science and Earth Research Institute, University of California, Santa Barbara, CA 93106, USA. [3]Isotope Laboratory, Department of Earth and Space Sciences, University of Washington, Seattle, WA 98195, USA.
*Correspondence author. Email: lsa@cugb.edu.cn

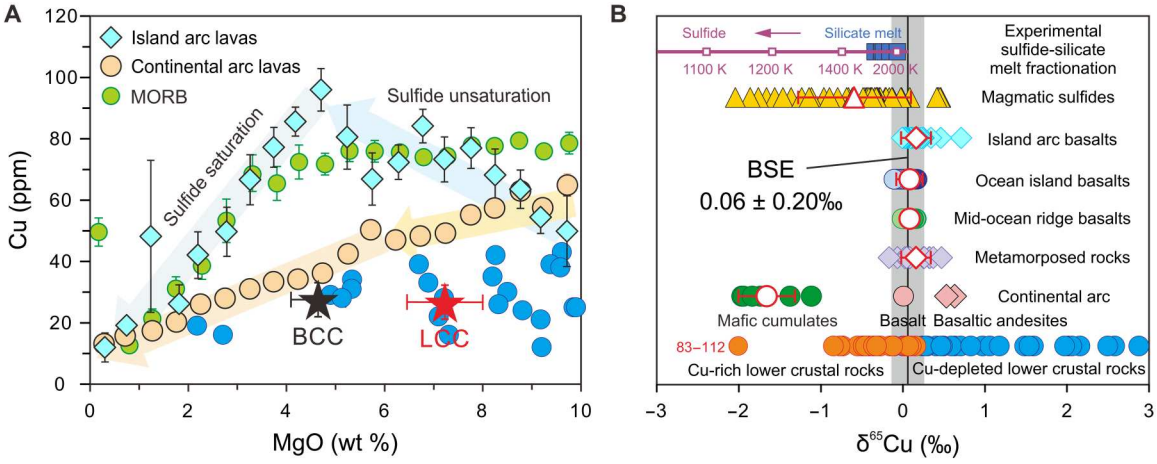

Fig. 1. Cu systematics of arc magmas and Cu isotopic systematics of terrestrial reservoirs. (**A**) [Cu] versus MgO in arc volcanic rocks and MORB. Individual symbols represent the average Cu and MgO contents of 1 wt % of MgO intervals with two SEs. Colored arrows represent sulfide saturation at MgO below 5 wt % and sulfide unsaturation at MgO over 5 wt %. MORB data are from (*28*). Data for global island and continental arc volcanic rocks (Cascades, Andes, and Mexico) are from the PetDB (https://search.earthchem.org/) and GEOROC databases (https://georoc.eu/georoc/). Data for bulk and LCC are from (*1*). The Cu-depleted lower crustal rocks are plotted for comparison. (**B**) Comparison of δ^{65}Cu values among lower crustal rocks, continental arc cumulates, basalt and basaltic andesites in southern Tibet, sulfides in magmatic Cu ore deposits (*19*, *20*, *78*), and various types of basalts (*16*, *17*, *27*, *28*, *79*). The equilibrium Cu isotope fractionation between sulfide and silicate melts is from the experimental work of (*21*). The average δ^{65}Cu values and SDs are given. The gray vertical band denotes the δ^{65}Cu of the bulk silicate Earth (BSE) (*16*).

foundering of sulfide-rich mafic cumulates cause the Cu depletion in the continental crust.

RESULTS

The lower crustal rocks are xenoliths from North Queensland (Australia) and both xenoliths and outcrops from Xuzhou-Bengbu (eastern China) and have variable chemical compositions (e.g., MgO, Cr, Ni, and Al_2O_3/CaO) falling about the globally averaged LCC composition (fig. S2). The lower crustal cumulates are from southern Tibet, represent tectonically uplifted products of intracrustal differentiation of continental arc magmas, and are thus considered to be compositionally complementary to the differentiated upper continental crust (UCC). The continental arc basalts and basaltic andesites are also from the Gangdese arc in southern Tibet. The metamorphosed rocks are from the Dabie-Sulu orogenic belt and experienced metamorphic grades ranging from greenschist facies through amphibolite facies to eclogite facies. Details of the geologic settings and sample descriptions can be found in Materials and Methods.

The lower crustal rocks are divided into Cu-depleted and Cu-rich subgroups based on a threshold [Cu] of ~50 ppm, which is close to that of primitive continental arc magmas [~50 to 60 ppm at 8 to 10 weight % (wt %) of MgO; Fig. 1A]. The Cu isotopic compositions of these rocks negatively correlate with their Cu abundances and range well beyond the δ^{65}Cu range of global arc basalts (Fig. 1B and table S1). The Cu-depleted lower crustal rocks are notably enriched in the heavier Cu isotope, while the Cu-rich lower crustal rocks generally have lighter Cu isotopic compositions than those of the mantle or the bulk silicate Earth (BSE) (Fig. 1B). Similar to the Cu-rich lower crustal rocks, the deep-seated arc cumulates from southern Tibet have high Cu contents of 392 to 2760 ppm and light Cu isotopic compositions with δ^{65}Cu values varying from −1.96 to −1.11‰ (Fig. 1B and table S1). The continental arc basalt from southern Tibet has a mantle-like δ^{65}Cu value of 0.01‰, whereas the basaltic andesites have higher δ^{65}Cu values of 0.53 to 0.63‰ (Fig. 1B and table S1). The Dabie-Sulu metamorphosed rocks have nearly identical [Cu] (5.4 to 42 ppm) and Cu isotopic compositions (−0.17 to 0.47‰) to one another regardless of their metamorphic grades (Fig. 1B and table S2).

DISCUSSION

Origins of copper isotopic variation in lower crustal rocks

The negative correlation between δ^{65}Cu and [Cu] in Cu-depleted rocks (Fig. 2A) is inconsistent with chemical weathering, alteration, or sulfide oxidative dissolution because these processes preferentially release heavy Cu into fluids and leave behind isotopically light residues (*24*–*26*). Elemental mapping reveals that Cu in the lower crustal xenoliths is dominantly hosted by chalcopyrite (fig. S3), also implying negligible redox breakdown of primary sulfides. Samples containing secondary sulfides formed by fluid/melt metasomatism may be enriched in heavy Cu isotopes, but these rocks are typically Cu-rich because of the addition of exotic Cu (*16*, *26*). This contradicts the overwhelmingly light Cu isotopic composition of the Cu-rich rocks (Fig. 2A), indicating that these sulfides are not metasomatic. Contamination of the xenoliths by the host magmas can also be excluded, given the mantle-like δ^{65}Cu values of the latter (table S1). The lack of correlation between δ^{65}Cu and Ba/Th and Ba/Nb (proxies for fluids; fig. S4) indicates negligible effects of metamorphic dehydration on the δ^{65}Cu in their igneous protoliths. Therefore, the Cu isotopic heterogeneity observed in the lower crustal granulites is primarily inherited from their igneous protoliths.

Most modern island arc lavas have mantle-like δ^{65}Cu values (Fig. 2A), regardless of their MgO contents, [Cu], and elemental ratios (e.g., Ba/Nb and Th/Yb) (*16*, *27*, *28*), including the

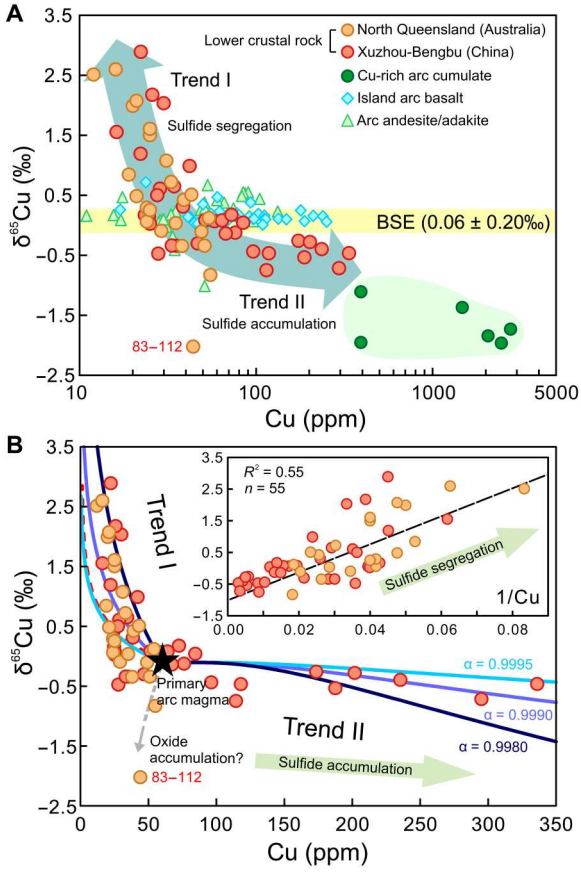

Fig. 2. Correlation between δ^{65}Cu and [Cu] for lower crustal rocks and sulfide-rich arc cumulates. δ^{65}Cu versus Cu contents in logarithmic (**A**) and linear coordinates (**B**), respectively. Two trends for lower crustal rocks are observed: trend I for Cu-depleted and high-δ^{65}Cu rocks and trend II for Cu-rich and low-δ^{65}Cu rocks. Arc cumulates follow the trend II. Original data are provided in table S1. The δ^{65}Cu data for granulite xenoliths from Hannuoba in the North China craton are not plotted because these rocks suffered strong oxidative sulfide breakdown and associated Cu mobilization (*26*). All data for arc basalts and andesites, including high-Mg andesites are from (*16*, *27*, *28*, *79*). The horizontal yellow band represents the δ^{65}Cu of BSE (*16*). The red dashed line represents sulfide fractionation along with 5% Fe-Ti oxides. Details of the Rayleigh fractionation models are given in Materials and Methods. Inset in (B) shows the correlation between δ^{65}Cu and 1/Cu (ppm^{-1}).

continental arc basalt from southern Tibet analyzed in this study (Fig. 1B), which suggests that there has been limited addition of slab-derived Cu to the subarc mantle. Our results from subduction-zone metamorphosed rocks support this interpretation and reveal a lack of systematic variation in both [Cu] and δ^{65}Cu values from greenschist to eclogite facies metamorphism, reflecting a minimal loss of Cu during slab dehydration (fig. S4). In addition, [Cu] of primary arc lavas is not distinctly different from that of MORB at similar MgO contents (Fig. 1A) (*29*). Primary arc lavas have Cu/Sc ratios, a proxy for Cu enrichment in mantle sources, that are also indistinguishable from those of MORB at given MgO (*6*). Although some metasomatized xenoliths from the continental lithospheric mantle exhibit a wide range of δ^{65}Cu values (*16*, *30*), these Cu-isotope signatures are not observed in island arc magmas (Fig. 1B). Thus, the large range of δ^{65}Cu observed in the lower crustal rocks is unlikely to be inherited from the mantle sources of their arc magma precursors. Instead, it likely formed by substantial isotopic fractionation during igneous differentiation.

The high δ^{65}Cu observed in Cu-depleted lower crustal rocks requires segregation of an isotopically light phase during magmatic differentiation. Because the equilibrium Cu isotope fractionation between silicate minerals (e.g., pyroxene) and silicate melt at magmatic temperatures is close to zero (*31*), sulfide is the best candidate for this phase. Although Fe-Ti oxide is also isotopically lighter than the basaltic melt (table S1), oxide fractionation has a weak influence on the melt composition (Fig. 2B, red dashed line) relative to sulfide fractionation because the partition coefficient of Cu betweenoxides and basaltic melts is three orders of magnitude lower than that between sulfides and basaltic melts (*6*, *32*). One lower crustal xenolith (83 to 112 from Chudleigh, North Queensland, Australia) has a low δ^{65}Cu value and falls off the trends defined by the other samples (Fig. 2); this sample contains unusually large amounts of cumulate Fe-Ti oxides (*33*), and its low δ^{65}Cu is most likely the result of oxide accumulation (Fig. 2B).

The average valence state of Cu in silicate melt varies between +1 and +2, increasing with elevated fO_2 of the melt (*34*), and reaches ~+1.76 at the fO_2 of typical arc magmas (+1.3 relative to the Fayalite-Magnetite-Quartz buffer) (*15*, *35*). Provided that monovalent Cu dominates in crystalline sulfide and sulfide melt (*36*–*38*), the equilibrium Cu isotope fractionation factor between sulfide and silicate melt ($\alpha^{65}Cu_{sulfide-silicate\ melt}$) is ~0.9990 to 0.9995 at 1100° to 1200°C—the temperature for early sulfide saturation in basaltic magmas (*39*); this value substantially reduces to ~0.9980 at ~950°C (fig. S5). Rayleigh fractionation modeling indicates that the heavy Cu isotopic composition and its negative correlation with [Cu] in the Cu-depleted rocks can be produced by sulfide fractionation from their igneous protoliths at a range of $\alpha^{65}Cu_{sulfide-silicate\ melt}$ values from ~0.9980 to 0.9995 (trend I; Fig. 2B). Thus, the Cu isotopic compositions of the Cu-depleted rocks were mainly controlled by sulfide fractionation, although some of the Cu-depleted rocks with extremely high δ^{65}Cu values (>~2‰) may have involved additional (~900°C) processes in the lower crust, such as reactive porous flow, redistribution of the magmatic sulfides, and/or subsolidus reequilibrium of sulfides (*40*, *41*). Despite the highly variable δ^{65}Cu values of Cu-depleted rocks, they are all complementary to the low δ^{65}Cu values of the Cu-rich lower crustal rocks and continental arc cumulates (Fig. 2); the latter two contain sulfide inclusions within silicate minerals or sulfides as intergranular phases (fig. S3), suggesting that their extremely light Cu isotopic compositions are the result of sulfide saturation and accumulation during differentiation of their igneous protoliths.

Sulfide fractionation and lower crustal foundering in making continental crust

The results presented here provide insights into the origin of the continental crust's Cu deficit, which is intrinsically associated with continental crust formation. Chemical weathering has been proposed to lead to depletion of Mg in the continental crust and may help convert basaltic arc crust into andesitic continental crust (*42*–*44*). Chemical weathering of sulfides can efficiently extract Cu from crustal rocks, but the gradual increase in δ^{65}Cu with lower [Cu] in the lower crustal rocks is opposite to that observed in weathering profiles, where redox transformation of Cu(I) in sulfides into Cu(II) in fluids preferentially leaves behind

isotopically light residues (*24*), suggesting that the Cu deficit in the continental crust is not the result of chemical weathering.

Instead, the negative correlation between δ^{65}Cu and [Cu] supports several previous studies suggesting that intracrustal sulfide fractionation in mantle-derived magmas exerts the main control on Cu systematics of crustal rocks (*6*, *7*, *12*, *13*). To explain the depletion of Cu in the upper and middle continental crust (MCC) (28 and 26 ppm on average, respectively) (*1*) relative to primary arc magmas (~50 to 60 ppm) (*13*) by accumulation of Cu-rich sulfides crystallizing in the lower crust, mass balance requires that the LCC has an average [Cu] of ~120 to 140 ppm (Fig. 3A). However, global lower crustal granulites have much lower [Cu] than this (Fig. 3A). Thus, Cu-rich cumulates must have been lost from the lower crust via density foundering or similar processes. To create a BCC having [Cu] of 27 ppm (*1*), mass balance indicates that the mass ratio of recycled lower crust to the modern continental crust is ~0.21 on average (fig. S6). Errors in estimating [Cu] of the recycled lower crust (196 ± 44 ppm; fig. S6) have considerable effect on the mass balance, but we are able to make an estimate based on Monte Carlo models. The remainder of the continental crust is estimated to have an average δ^{65}Cu value of 0.30 ± 0.15‰ (Fig. 3B). Thus, intracrustal differentiation leads to a Cu-depleted BCC that is slightly isotopically heavier than the mantle due to the net removal of isotopically light sulfides via lower crustal foundering.

The lower crustal rocks investigated here display a broadly positive correlation between δ^{65}Cu and SiO_2 and a negative correlation with MgO (fig. S7), further supporting the conclusion that more differentiated crustal rocks have heavier Cu isotopic composition. Because Cu is highly incompatible in silicate minerals (*14*), these correlations suggest the removal of sulfides, along with mafic minerals during intracrustal differentiation. Accumulation of sulfide-rich mafic/ultramafic lithologies in deep continental crust and arcs, as observed in continental arc cumulates from southern Tibet (this study), Arizona, and the Sierra Nevada (*6*, *13*), would cause differentiated magmas to be depleted in both Cu and Mg and have higher δ^{65}Cu values. Subsequent removal of these mafic/ultramafic cumulates from the continental crust through density foundering (*4*–*6*) generates the Cu-depleted, slightly isotopically heavy, andesitic BCC (Fig. 4). This model can also explain the deficit of other chalcophile metals (e.g., Ag, Au, and Pb) in the continental crust compared to primary arc magmas (*7*).

Arc magmas erupting through thin crust (e.g., Tonga, Izu-Bonin-Marianas, and Kamchatka; <25 km in thickness) (*45*, *46*) exhibit a narrow range of δ^{65}Cu values over a broad range of [Cu] (Fig. 2A). This suggests no apparent Cu isotope fractionation during sulfide segregation of these magmas (*27*). By contrast, strong Cu isotope fractionation is seen in the extremely low-δ^{65}Cu lower crustal mafic cumulates and in evolved basaltic andesites with δ^{65}Cu values that are up to 0.6‰ higher than those of the basalt (table S1) from southern Tibet where the arc crust is at least 40 to 50 km in thickness (*47*). This is consistent with experimental studies showing that sulfides in deep-crustal cumulates have enhanced stability with increasing pressure (*48*), allowing Cu-rich sulfides to crystallize at high pressures (HPs) (1.0 to 1.5 GPa) even from relatively oxidized magmas and then accumulate in the deep arc. Moreover, sulfide-rich arc cumulates in the deep continental crust may be subject to reactive melt flow and mobilization of magmatic sulfides as discussed above (*40*, *41*). These differences at least partly explain the more variable δ^{65}Cu values seen in the lower crustal cumulates and the basaltic andesites from Tibet. Given that the Cu isotopic variations of lower crustal rocks exceed the range observed in arc magmas erupted in thin arcs, our findings strongly support the view that arc magmas traversing thick (continental) crust are responsible for generating mature continental crust (*13*, *49*). Last, the Cu isotopic compositions of lower crustal rocks exceed those of andesites in modern arcs (Fig. 2A), suggesting that it is unlikely that andesites dominate post-Archaean continental crustal growth without further intracrustal differentiation.

Implications for porphyry copper systems

Understanding the fate of Cu during intracrustal differentiation has implications for the origins of porphyry copper systems. Some studies have suggested that subducted slabs bring oxidized fluids to the mantle wedge, leading to the formation of oxidized arc magmas and porphyry Cu systems along convergent plate boundaries (*8*, *50*, *51*). These slab-derived oxidized fluids can also transport Cu and other chalcophile metals to the subarc mantle (*52*, *53*). In these fluids, Cu complexation with sulfate species incorporates heavy over light Cu isotopes (*23*). However, the constant Cu

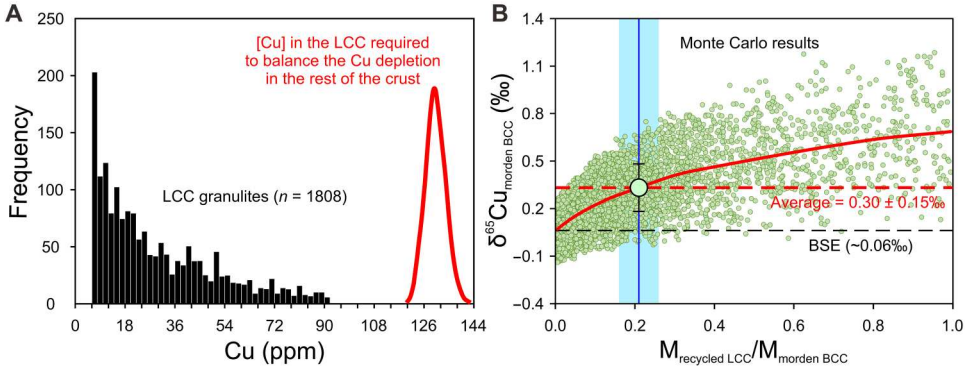

Fig. 3. Modeling recycled LCC. (**A**) Histogram of the distribution of [Cu] in LCC granulite facies rocks and [Cu] in the LCC required to balance the Cu depletion of UCC and MCC in the absence of delamination. Data for LCC granulites (*n* = 2212) are from Earthchem.org (http://www.EarthChem.org/). We excluded 20% of the samples with highest and lowest [Cu] to reduce the chance of incorporating atypical samples or bad analyses. (**B**) δ^{65}Cu of the modern BCC versus the mass proportion of recycled LCC. The solid lines denote the average result of Rayleigh distillation. Details of the Monte Carlo and Rayleigh fractionation models are given in Materials and Methods.

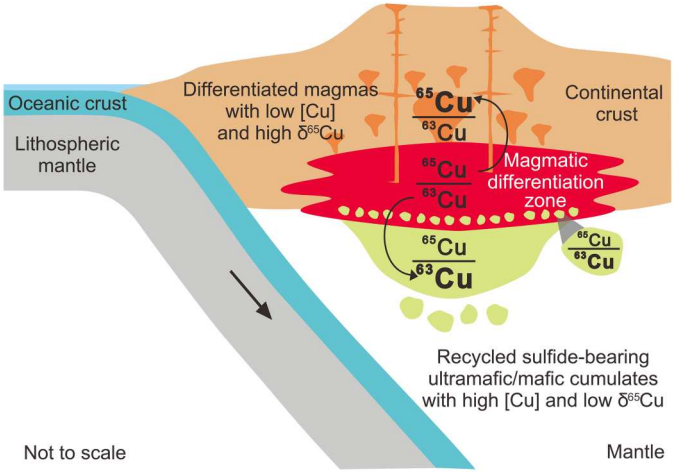

Fig. 4. Schematic model for intracrustal sulfide fractionation. Sulfide fractionation during intracrustal differentiation of mantle-derived magmas results in enrichment of the lighter Cu isotopes in Cu-rich lower crustal rocks and continental arc cumulates, leaving behind differentiated magmas characterized by low [Cu] and high δ^{65}Cu. Foundering of dense, Cu-rich mafic/ultramafic cumulates from the lower crust leaves the continental crust depleted in both Cu and Mg.

isotopic compositions observed in subduction-zone rocks metamorphosed at different grades (fig. S4) suggest that Cu is not strongly incorporated into sulfate species during slab dehydration. Together with the similar [Cu] and Cu/Sc ratios between primary arc lavas and MORB at given MgO (*6*), these observations suggest that pre-enrichment of Cu in the subarc mantle by oxidized slab fluids is not important in the formation of porphyry Cu systems. This conclusion is consistent with a sulfur isotope study that also suggests limited contribution of slab sulfate to the mantle sources of arc lavas (*54*). Instead, large magma volumes and prolonged magmatic activity play critical roles in the formation of porphyry Cu systems in thick (continental) arcs (*55*, *56*). In addition, continental arc cumulates from southern Tibet, where giant porphyry Cu ore deposits are widespread (*57*, *58*), are dominated by hornblende-bearing assemblages (*47*). Hydrous magmas derived from these cumulates would enhance the ability of endogenic fluids to extract Cu from felsic magmas, which further promotes the formation of porphyry Cu systems.

MATERIALS AND METHODS

Lower crustal rocks

Two types of rocks are available from the LCC: granulite xenoliths and high-grade metamorphic terranes. Granulite xenoliths from the McBride and Chudleigh volcanic provinces, North Queensland, Australia, are hosted by Cenozoic basalts (fig. S1) and are predominantly mafic in composition with minor felsic to intermediate lithologies in McBride (*33*, *59*). The protoliths of several McBride xenoliths formed at ~1.57 Ga, while most formed at 300 Ma (*59*). All McBride xenoliths underwent granulite facies metamorphism at 300 Ma, followed by slow cooling in the lower crust (*59*). The Chudleigh xenoliths are plagioclase-rich and pyroxene-rich granulites. Chemical and isotopic compositions (O, Sr, Nd, Hf, Pb, and Os) indicate that the Chudleigh xenoliths are cogenetic crystal cumulates derived from mafic magmas (*33*, *60*–*63*). Samples analyzed in this study have been previously used to assess the composition of the LCC and were well characterized in terms of petrology and geochemistry [e.g., (*33*, *59*, *64*)]. All samples are relatively fresh, and alteration is generally restricted to grain boundary zones or in development of kelyphite on garnet. Lower crustal rocks exposed as xenoliths within early Cretaceous intrusions (dioritic porphyry) and as bands or lenses in the Precambrian metamorphic basement in the Xuzhou-Bengbu area of the North China craton (fig. S1) are mainly mafic, including garnet granulites and garnet amphibolites, composed of garnet, clinopyroxene, Ti-rich amphibole, plagioclase, and quartz with minor rutile, ilmenite, and sphene, and several samples are plagioclase amphibolites. These xenoliths and terranes are predominantly mafic and underwent HP granulite facies metamorphism at ~1.8 Ga with protolith ages of ca. 2.5 to 2.4 Ga (*65*). Geochemical data (e.g., Nb and Ta depletion) and hydrous characteristic indicate that their protoliths resemble mafic igneous rocks formed at convergent continental margin arc setting (*66*). More detailed descriptions can be found in (*65*–*67*). Given that these rocks dominantly formed at arc settings, there is no geodynamic difference between the Cu-rich and Cu-depleted subgroups, but they display systematic differences in chemical compositions (e.g., MgO and SiO_2) in addition to Cu isotopes (fig. S7).

Collectively, the lower crustal samples investigated here show a negative correlation between MgO with Al_2O_3/CaO and positive correlation between MgO with Cr and Ni contents (fig. S2). These correlations suggest that their igneous protoliths underwent varying degrees of fractional crystallization and accumulation. Some of the lower crustal xenoliths from Xuzhou-Bengbu are considerably Cu-rich (up to ~350 ppm) and contain sulfides (chalcopyrite, pyrrhotite, and pyrite) included within silicate minerals or occurring at grain boundaries (fig. S3), suggesting sulfide accumulation during differentiation of their igneous protoliths.

Continental arc cumulates, basalts, and basaltic andesites

The Gangdese arc in southern Tibet is a juvenile continental magmatic arc formed by Mesozoic subduction of the Neo-Tethyan oceanic lithosphere and Cenozoic collision between the Indian and Asian continents (fig. S1) and has been extensively studied in recent years [e.g., (*47*, *68*, *69*)]. The exposed lower arc crustal section of the Gangdese arc consists mainly of garnet gabbros (*68*), which crystallized at the base of the continental arc root and formed as typical cumulates by intracrustal differentiation of the late Mesozoic hydrous basaltic arc magmas (*47*). These lower crustal cumulates underwent HP (1.3 to 1.7 GPa) granulite facies metamorphism, suggesting an arc crustal thickness of at least 40 to 50 km (*47*). One of the most noticeable characteristics of the Gangdese mafic cumulates is the high abundance of sulfides and the strong enrichment of Cu (up to >1000 ppm) (*47*). These rocks also contain a considerable amount of amphibole along with garnet that formed during differentiation of arc magmas in the lowermost portion of thick crust (*70*). The sulfide-rich mafic cumulates in this study were collected from Linzhi in the Gangdese arc (fig. S1). Pyrrhotite is the dominant Cu-rich sulfide in these cumulates, with minor pyrite and chalcopyrite (fig. S3), which is similar to the assemblage of sulfides in continental arc cumulates (garnet pyroxenites) from the Sierra Nevada batholith and Arizona (*6*, *13*). The calc-alkaline basalts and basaltic andesites are from Pangduo in the Gangdese arc (fig. S1). These rocks display typical arc-lava geochemical features and were derived from a subarc mantle source associated with northward

subduction of the Neo-Tethyan oceanic slab (*71*), with different chemical compositions reflecting magma evolution.

Subduction-zone metamorphosed rocks

The metamorphosed rocks in the Dabie-Sulu orogenic belt formed during northward subduction of basaltic crust of the South China Block and its final collision with the North China Block in the Triassic (fig. S1). Rocks investigated include Neoproterozoic mafic volcanic rocks (unmetamorphosed protoliths), amphibolites, and eclogites. These are ideal samples with which to investigate the behavior of elements and isotopes during metamorphic dehydration of basaltic rocks in a subduction zone (*72*). The amphibolites contain amphibole + clinopyroxene + plagioclase + biotite + epidote + quartz + calcite. Eclogites occur as fresh blocks or lenses within gneisses, marbles, and ultramafic massifs, and the dominant minerals are garnet and clinopyroxene. Coesite and/or diamond inclusions preserved in zircons and garnets indicate that the basaltic protoliths of these eclogites were subducted to depths of at least 90 to 120 km (*73*) and experienced peak metamorphism at temperatures of ~650 to 750°C. More detailed information can be found in (*72*).

Elemental mapping

To determine the distribution of Cu and identify the major hosts for Cu in lower crustal rocks, we performed elemental mapping using the TESCAN Integrated Mineral Analyzer (TIMA). After carbon coating, two well-polished probe slices (samples 14JG-35 and 20JG-16, with Cu contents of 188 and 177 ppm, respectively) were loaded and scanned in the TIMA-3 analyzer. The raw data were imported and processed using software TESCAN TIMA version 2.7.0. By comparison with the standard mineral dataset (www.webmineral.com), the proportion of unclassified mineral phases is less than ~5%. Field 155 in 14JG-35 and field 117 in 20JG-16 including BSE and element mapping images are shown in fig. S3. Copper (Cu) and sulfur (S) elemental mapping is shown in magenta and brown colors, respectively. The numbers in fig. S3 represent signal intensities in energy spectrum. This number is semiquantitative and does not correspond to parts per million.

Copper isotope analysis

About 1 to 20 mg of powder of each sample was digested in a 1:1 concentrated HF:HNO_3 mixture at 160°C in perfluoroalkoxy beakers. After complete dissolution, the sample was transferred into 1 ml of 8 N HCl + 0.001% H_2O_2 in preparation for ion-exchange separation. Each sample was loaded through a column containing precleaned strong anion resin (AG-MP-1M), following the procedures outlined in (*74*, *75*) to separate Cu from matrices. The U.S. Geological Survey basalt standards (BIR-1, BHVO-2, and BCR-2) were also processed through column chemistry. The recovery of Cu is 99.5 ± 0.8% (2SD). The total procedural blank is <2 ng, and, thus, no blank corrections were performed. The purified Cu fractions were lastly dissolved in 3% (*m*/*m*) HNO_3 for isotope analysis. The presence of Ti and Na in the solution was checked for each purified sample owing to their potential interference contribution at ^{63}amu and ^{65}amu. After two passes of column chemistry, these elements are low enough to be negligible (molar Ti/Cu < 0.005 and Na/Cu < 0.001) for all studied samples. Isotope ratio measurements were conducted on a Thermo-Finnigan Neptune Plus multiple-collector inductively coupled plasma mass spectrometer at the Isotope Geochemistry Lab of the China University of Geosciences, Beijing. Instrumental mass fractionation of Cu isotopes was corrected by a combination of standard-sample bracketing and elemental doping by adding a Zn isotopic reference (IRMM 3702) to each sample based on the exponential law (*74*). Copper isotope data are reported in the standard notation in per mil relative to the standard reference material NIST 976

$$\delta^{65}Cu = [(^{65}Cu/^{63}Cu)_{sample}/(^{65}Cu/^{63}Cu)_{NIST\ 976} - 1] \times 1000$$

The long-term external reproducibility of δ^{65}Cu is ±0.05‰ (2SD) obtained by repeat analyses of natural samples and synthetic solutions (*75*). Each sample was measured three times, and the average is reported. The Cu isotopic compositions of three basalt standards analyzed during the course of this study overlap with the recommended values within uncertainty (table S1) (*23*).

Sulfide fractionation model

To quantify the extent of Cu isotope fractionation during sulfide fractionation or accumulation from silicate magmas, we adopted the Rayleigh fractionation models as follows

$$[Cu]_{silicate\ melt} = [Cu]_0 \times F^{(D-1)} \quad (1)$$

$$\delta^{65}Cu_{silicate\ melt} = (\delta^{65}Cu_0 + 1000) \times f^{(\alpha-1)} - 1000 \quad (2)$$

$$\delta^{65}Cu_{cumulate} = (\delta^{65}Cu_0 + 1000) \times (1 - f^{\alpha})/(1 - f) - 1000 \quad (3)$$

where α is the equilibrium Cu isotope fractionation factor between sulfide and silicate melt based on experimental work at 1.5 GPa (*21*), F is the mass fraction of evolving silicate melt, and f [$(1 - F) \times [Cu]_{silicate\ melt}/[Cu]_0$] is the mass fraction of Cu remaining in the melt with an initial [Cu] of ~60 ppm, close to that of primary continental arc lavas (*13*) and Cu isotopic composition ($\delta^{65}Cu_0$) of 0.06‰ equal to that of the BSE (*16*). In equilibrium with silicate melt, sulfide with high Ni content (~25 wt %) exhibits larger Cu isotope fractionation than that with low Ni content (<1.2 wt %) (*21*); sulfides in the investigated samples have low Ni content (<0.2 wt %), and, thus, the low Ni experimental result of (*21*) is applied, which gives α values between 0.9995 and 0.9980 at a temperature range of ~1200 to 950°C and in fO_2 of typical arc magmas (fig. S5). The partition coefficients of Cu (D) between clinopyroxene, garnet, and sulfide and melt are 0.043, 0.0035, and 800, respectively (*6*). The mineral mass fraction is assumed to be 0.79, 0.20, and 0.01 for clinopyroxene, garnet, and sulfide, respectively. The sulfide fraction (~1 wt %) used in this model falls within the range of sulfide fractions observed in deep crustal cumulates [(*6*, *76*), this study]. Other parameters can be obtained by mass conservation. The modeling results are plotted in Fig. 2B. The negative correlation between δ^{65}Cu and [Cu] in the Cu-depleted lower crustal rocks (trend I) can be generated by sulfide segregation from a primary magma with an initial [Cu] of ~60 ppm at a range of α values from ~0.9980 to 0.9995. The high Cu contents and light Cu isotopic compositions of the Cu-rich lower crustal rocks and continental arc cumulates are modeled via sulfide accumulation from primary mantle-derived magmas at similar $\alpha^{65}Cu_{sulfide\text{-}melt}$ values (trend II).

The potential role of oxide fractionation or accumulation in the Cu isotopic composition of magmas is also plotted in Fig. 2B. The red dashed line represents fractional crystallization of sulfides along with 5% Fe-Ti oxides at 1300 K. The $\alpha^{65}Cu_{oxide\text{-}melt}$ value is assumed to be ~0.999 based on the apparent Cu isotope fractionation between Fe-Ti oxide and the host basalt (table S1). The partition coefficient of Cu between oxide and basaltic melt is 0.79 (*32*).

Modeling the proportion of recycled lower crust

In the absence of delamination, the Cu content of the LCC required to reconcile the depletion of Cu in the UCC and MCC can be estimated by adopting the following equations

$$[Cu]_{JCC} \times m_{JCC} = [Cu]_{LCC} \times m_{LCC} + [Cu]_{MCC} \times m_{MCC} + [Cu]_{UCC} \times m_{UCC} \quad (4)$$

$$m_{JCC} = m_{LCC} + m_{MCC} + m_{UCC} \quad (5)$$

$$[Cu]_{LCC} = ([Cu]_{JCC} \times m_{JCC} - [Cu]_{MCC} \times m_{MCC} - [Cu]_{UCC} \times m_{UCC})/(m_{JCC} - m_{MCC} - m_{UCC}) \quad (6)$$

where the mass proportions of LCC, MCC, and UCC are based on global seismic data in (*77*). The [Cu] of the UCC and MCC are from (*1*), and the [Cu] of the juvenile continental crust is assumed to be ~50 to 60 ppm, close to that of primary continental arc magmas (*13*). Using a Monte Carlo scheme with kernel density estimation, the modern LCC is required to contain ~120 to 140 ppm Cu to create a bulk crust having similar [Cu] to primitive arc magmas (Fig. 3A), following Eq. 6. However, the modern BCC has a much lower [Cu] of ~27 ppm on average (*1*), Thus, Cu-rich cumulates must have been recycled into the mantle via density foundering or similar processes. Below, we use the same method to calculate the mass proportion of recycled, Cu-rich lower crust as follows

$$[Cu]_{JCC} \times m_{JCC} = [Cu]_{recycled\ LCC} \times m_{recycled\ LCC} + [Cu]_{modern\ BCC} \times m_{modern\ BCC} \quad (7)$$

$$m_{JCC} = m_{recycled\ LCC} + m_{modern\ BCC} \quad (8)$$

$$\frac{m_{recycled\ LCC}}{m_{modern\ BCC}} = \frac{[Cu]_{JCC} - [Cu]_{modern\ BCC}}{[Cu]_{recycled\ LCC} - [Cu]_{JCC}} \quad (9)$$

where [Cu] of the modern BCC is from (*1*) and [Cu] of the recycled LCC is represented by lower crustal cumulates (*13*, *47*), which have an average [Cu] of 196 ± 44 ppm (n = 166). A histogram of Cu contents in lower crustal cumulates is provided in fig. S6. To match the juvenile continental crust composition ([Cu] = 50 to 60 ppm), Monte Carlo simulations indicate that the mass ratio of recycled LCC to the modern BCC is 0.21 ± 0.05 (fig. S6) based on Eq. 9.

On this basis, we use a Rayleigh fractionation model to estimate the Cu isotopic composition of the modern BCC, i.e., the BCC left behind after lower crustal foundering, as follows

$$\delta^{65}Cu_{modern\ BCC} = (\delta^{65}Cu_{JCC} + 1000) \times f^{(\alpha-1)} - 1000 \quad (10)$$

where α is the Cu isotope fractionation factor between recycled LCC and primary arc magmas at temperatures of 1100° to 1200°C, which is assumed to vary between 0.9995 and 0.9999 depending on the amount of sulfide in the recycled LCC, and f is the mass fraction of Cu remaining in the continental crust after foundering, expressed as

$$f = 1/\left(\frac{[Cu]_{recycled\ LCC} \times m_{recycled\ LCC}}{[Cu]_{modern\ BCC} \times m_{modern\ BCC}} + 1\right) \quad (11)$$

The Cu isotopic composition of the juvenile continental crust ($\delta^{65}Cu_{JCC}$) is taken to be 0.06 ± 0.20‰, equal to that of primary arc magmas and the BSE (*16*). The average modeling results and Monte Carlo simulations are plotted in Fig. 3B. While the extremely high δ^{65}Cu values of some of the Cu-depleted lower crustal rocks may have involved additional lower crustal processes at ~950°C, these processes do not affect the estimate of δ^{65}Cu in the differentiated crust because the adopted isotope fractionation factor is ≥0.9995, which corresponds to temperatures for early sulfide saturation in basaltic melts (1100° to 1200°C) (*39*). The modern BCC is then estimated to have an average δ^{65}Cu of 0.30 ± 0.15‰. As the proportion of recycled LCC increases, the δ^{65}Cu of the remaining continental crust gradually increases.

Supplementary Materials

This PDF file includes:

Figs. S1 to S7
Tables S1 and S2
References

REFERENCES AND NOTES

1. R. L. Rudnick, S. Gao, Composition of the continental crust, in *Treatise on Geochemistry (1st ed)*, H. D. Holland, K. K. Turekian, Eds. (Pergamon, 2003), pp. 1–64.
2. A. T. Anderson, Parental basalts in subduction zones: Implications for continental evolution. *J. Geophys. Res.* **87**, 7047–7060 (1982).
3. S. R. Taylor, S. M. McLennan, Eds., *The Continental Crust: Its Composition and Evolution* (Blackwell, 1985).
4. R. W. Kay, S. Mahlburg-Kay, Creation and destruction of lower continental crust. *Geol. Rundsch.* **80**, 259–278 (1991).
5. R. L. Rudnick, Making continental crust. *Nature* **378**, 571–578 (1995).
6. C.-T. A. Lee, P. Luffi, E. J. Chin, R. Bouchet, R. Dasgupta, D. M. Morton, V. Le Roux, Q.-Z. Yin, D. Jin, Copper systematics in arc magmas and implications for crust-mantle differentiation. *Science* **336**, 64–68 (2012).
7. F. E. Jenner, Cumulate causes for the low contents of sulfide-loving elements in the continental crust. *Nat. Geosci.* **10**, 524–529 (2017).
8. R. H. Sillitoe, Porphyry copper systems. *Econ. Geol.* **105**, 3–41 (2010).
9. D. Cooke, P. Hollings, J. L. Walshe, Giant porphyry deposits: Characteristics, distribution, and tectonic controls. *Econ. Geol.* **100**, 801–818 (2005).
10. P. B. Kelemen, Genesis of high Mg# andesites and the continental crust. *Contrib. Mineral. Petrol.* **120**, 1–19 (1995).
11. C. J. Hawkesworth, A. I. S. Kemp, Using hafnium and oxygen isotopes in zircons to unravel the record of crustal evolution. *Chem. Geol.* **226**, 144–162 (2006).
12. M. Chiaradia, Copper enrichment in arc magmas controlled by overriding plate thickness. *Nat. Geosci.* **7**, 43–46 (2014).
13. K. Chen, M. Tang, C.-T. A. Lee, Z. C. Wang, Z. Q. Zou, Z. C. Hu, Y. S. Liu, Sulfide-bearing cumulates in deep continental arcs: The missing copper reservoir. *Earth Planet. Sci. Lett.* **531**, 1–9 (2020).
14. S. A. Fellows, D. Canil, Experimental study of the partitioning of Cu during partial melting of Earth's mantle. *Earth Planet. Sci. Lett.* **337-338**, 133–143 (2012).
15. S.-Y. Zhao, A. Y. Yang, C. H. Langmuir, T. P. Zhao, Oxidized primary arc magmas: Constraints from Cu/Zr systematics in global arc volcanics. *Sci. Adv.* **8**, 1–9 (2022).
16. S.-A. Liu, J. Huang, J. G. Liu, G. Wörner, W. Yang, Y.-J. Tang, Y. Chen, L. M. Tang, J. P. Zheng, S. G. Li, Copper isotopic composition of the silicate Earth. *Earth Planet. Sci. Lett.* **427**, 95–103 (2015).

17. P. S. Savage, F. Moynier, H. Chen, G. Shofner, J. Siebert, J. Badro, I. S. Puchtel, Copper isotope evidence for large-scale sulphide fractionation during Earth's differentiation. *Geochem. Persp. Let.* **1**, 53–64 (2015).
18. Z. Zhang, M. M. Hirschmann, Experimental constraints on mantle sulfide melting up to 8 GPa. *Am. Mineral.* **101**, 181–192 (2016).
19. K. N. Malitch, R. M. Latypov, I. Y. Badanina, S. F. Sluzhenikin, Insights into ore genesis of Ni-Cu-PGE sulfide deposits of the Noril'sk Province (Russia): Evidence from copper and sulfur isotopes. *Lithos* **204**, 172–187 (2014).
20. Y. Zhao, C. J. Xue, S.-A. Liu, D. T. A. Symons, X. B. Zhao, Y. Q. Yang, J. J. Ke, Copper isotope fractionation during sulfide-magma differentiation in the Tulaergen magmatic Ni–Cu deposit, NW China. *Lithos* **286-287**, 206–215 (2017).
21. Y. Xia, E. S. Kiseeva, J. Wade, F. Huang, The effect of core segregation on the Cu and Zn isotope composition of the silicate Moon. *Geochem. Persp. Let.* **12**, 12–17 (2019).
22. S. Liu, Y. Li, J. Liu, Z. Yang, J. Liu, Y. Shi, Equilibrium cu isotope fractionation in copper minerals: A first-principles study. *Chem. Geol.* **564**, 120060 (2021).
23. F. Moynier, D. Vance, T. Fujii, P. Savage, The isotope geochemistry of zinc and copper. *Rev. Mineral. Geochem.* **82**, 543–600 (2017).
24. R. Mathur, L. Jin, V. Prush, J. Paul, C. Ebersole, A. Fornadel, J. Z. Williams, S. Brantley, Cu isotopes and concentrations during weathering of black shale of the Marcellus formation, Huntingdon County, Pennsylvania (USA). *Chem. Geol.* **304-305**, 175–184 (2012).
25. S.-A. Liu, F.-Z. Teng, S. G. Li, G.-J. Wei, J.-L. Ma, D. D. Li, Copper and iron isotope fractionation during weathering and pedogenesis: Insights from saprolite profiles. *Geochim. Cosmochim. Acta* **146**, 59–75 (2014).
26. G. L. Zhang, Y. S. Liu, F. Moynier, Z. C. Hu, Y. T. Zhu, X. Jiang, M. Li, Copper mobilization in the lower continental crust beneath cratonic margins, a Cu isotope perspective. *Geochim. Cosmochim. Acta* **322**, 43–57 (2022).
27. Z. C. Wang, J.-W. Park, X. Wang, Z. Q. Zou, J. Kim, P. Y. Zhang, M. Li, Evolution of copper isotopes in arc systems: Insights from lavas and molten sulfur in Niuatahi volcano, Tonga rear arc. *Geochim. Cosmochim. Acta* **250**, 18–33 (2019).
28. Z. C. Wang, P. Y. Zhang, Y. B. Li, T. Ishii, W. Li, S. Foley, X. Wang, X. Wang, M. Li, Copper recycling and redox evolution through progressive stages of oceanic subduction: Insights from the Izu-Bonin-Mariana forearc. *Earth Planet. Sci. Lett.* **574**, 1–14 (2021).
29. F. E. Jenner, H. C. O'Neill, R. J. Arculus, J. A. Mavrogenes, The magnetite crisis in the evolution of arc-related magmas and the initial concentration of Au, Ag and Cu. *J. Petrol.* **51**, 2445–2464 (2010).
30. P. D. Kempton, R. Mathur, R. S. Harmon, A. Bell, J. Hoefs, B. Shaulis, Cu-isotope evidence for subduction modification of lithospheric mantle. *Geochem. Geophys. Geosyst.* **23**, (2022).
31. J. Huang, S.-A. Liu, G. Worner, H. M. Yu, Y. L. Xiao, Copper isotope behavior during extreme magma differentiation and degassing: A case study on Laacher See phonolite tephra (East Eifel, Germany). *Contrib. Mineral. Petrol.* **171**, 1–16 (2016).
32. T. Zack, R. Brumm, Ilmenite/liquid partition coefficients of 26 trace elements determined through ilmenite/clinopyroxene partitioning in garnet pyroxenites. *International Kimberlite Conference: Extended Abstracts* **7**, 986–988 (1998).
33. R. L. Rudnick, W. F. McDonough, M. T. McCulloch, S. R. Taylor, Lower crustal xenoliths from Queensland, Australia: Evidence for deep crustal assimilation and fractionation of continental basalts. *Geochim. Cosmochim. Acta* **50**, 1099–1115 (1986).
34. E. M. Ripley, J. G. Brophy, Solubility of copper in a sulfur-free mafic melt. *Geochim. Cosmochim. Acta* **59**, 5027–5030 (1995).
35. X. C. Liu, X. L. Xiong, A. Audétat, Y. Li, M. S. Song, L. Li, W. D. Sun, X. Ding, Partitioning of copper between olivine, orthopyroxene, clinopyroxene, spinel, garnet and silicate melts at upper mantle conditions. *Geochim. Cosmochim. Acta* **125**, 1–22 (2014).
36. A. Holzheid, K. Lodders, Solubility of copper in silicate melts as function of oxygen and sulfur fugacities, temperature, and silicate composition. *Geochim. Cosmochim. Acta* **65**, 1933–1951 (2001).
37. A. Lanzirotti, L. Lee, E. Head, S. R. Sutton, M. Newville, M. McCanta, A. H. Lerner, P. J. Wallace, Direct measurements of copper speciation in basaltic glasses: Understanding the relative roles of sulfur and oxygen in copper complexation in melts. *Geochim. Cosmochim. Acta* **267**, 164–178 (2019).
38. G. A. Gaetani, T. L. Grove, Partitioning of moderately siderophile elements among olivine, silicate melt, and sulfide melt: Constraints on core formation in the Earth and Mars. *Geochim. Cosmochim. Acta* **61**, 1829–1846 (1997).
39. J. W. Park, I. H. Campbell, J. Kim, J. W. Moon, The role of late sulfide saturation in the formation of a Cu-and Au-rich magma: Insights from the platinum group element geochemistry of Niuatahi–Motutahi lavas. *Tonga rear arc. J. Petrol.* **56**, 59–81 (2015).
40. M. D. Jackson, J. Blundy, R. S. J. Sparks, Chemical differentiation, cold storage and remobilization of magma in the Earth's crust. *Nature* **564**, 405–409 (2018).
41. D. A. Holwell, M. L. Fiorentini, T. R. Knott, I. McDonald, D. E. Blanks, M. T. Campbell, W. Gorczyk, Mobilisation of deep crustal sulfide melts as a first order control on upper lithospheric metallogeny. *Nat. Commun.* **13**, 573 (2022).
42. F. Albarède, A. Michard, Transfer of continental Mg, S, O, and U to the mantle through hydrothermal alteration of the oceanic crust. *Chem. Geol.* **57**, 1–15 (1986).
43. C.-T. A. Lee, D. M. Morton, M. G. Little, R. Kistler, U. N. Horodyskyj, W. P. Leeman, A. Agranier, Regulating continent growth and composition by chemical weathering. *Proc. Natl. Acad. Sci. U.S.A.* **105**, 4981–4986 (2008).
44. X.-M. Liu, R. L. Rudnick, Constraints on continental crustal mass loss via chemical weathering using lithium and its isotopes. *Proc. Natl. Acad. Sci. U.S.A.* **108**, 20873–20880 (2011).
45. G. Zellmer, Some first-order observations on magma transfer from mantle wedge to upper crust at volcanic arcs. *Geol. Soc. Lond. Spec. Publ.* **304**, 15–31 (2008).
46. E. Contreras-Reyes, I. Grevemeyer, A. B. Watts, E. R. Flueh, C. Peirce, S. Moeller, C. Papenberg, Deep seismic structure of the Tonga subduction zone: Implications for mantle hydration, tectonic erosion, and arc magmatism. *J. Geophys. Res.* **116**, B10103 (2011).
47. Z.-M. Zhang, H.-X. Ding, X. Dong, Z.-L. Tian, R. M. Palin, M. Santosh, Y.-F. Chen, Y.-Y. Jiang, S.-K. Qin, D.-Y. Kang, W.-T. Li, The Mesozoic magmatic, metamorphic, and tectonic evolution of the eastern Gangdese magmatic arc, southern Tibet. *Geol. Soc. Am. Bull.* **134**, 1721–1740 (2021).
48. V. Matjuschkin, J. D. Blundy, R. A. Brooker, The effect of pressure on Sulphur speciation in mid- to deep-crustal arc magmas and implications for the formation of porphyry copper deposits. *Contrib. Mineral. Petrol.* **171**, 1–25 (2016).
49. M. Tang, M. Erdman, G. Eldridge, C.-T. A. Lee, The redox "filter" beneath magmatic orogens and the formation of continental crust. *Sci. Adv.* **4**, 1–7 (2018).
50. K. A. Kelley, E. Cottrell, Water and the oxidation state of subduction zone magmas. *Science* **325**, 605–607 (2009).
51. J. P. Richards, Magmatic to hydrothermal metal fluxes in convergent and collided margins. *Ore Geol. Rev.* **40**, 1–26 (2011).
52. J. E. Mungall, Roasting the mantle: Slab melting and the genesis of major Au and Au-rich Cu deposits. *Geology* **30**, 915–918 (2002).
53. B. I. A. McInnes, J. S. McBride, N. J. Evans, D. D. Lambert, A. S. Andrew, Osmium isotope constraints on ore metal recycling in subduction zones. *Science* **286**, 512–516 (1999).
54. C.-T. A. Lee, M. Erdman, W. B. Yang, L. Ingram, E. J. Chin, D. J. DePaolo, Sulfur isotopic compositions of deep arc cumulates. *Earth Planet. Sci. Lett.* **500**, 76–85 (2018).
55. M. Chiaradia, L. Caricchi, Stochastic modelling of deep magmatic controls on porphyry copper deposit endowment. *Sci. Rep.* **7**, 44523 (2017).
56. J. W. Park, I. H. Campbell, M. Chiaradia, H. Hao, C. T. Lee, Crustal magmatic controls on the formation of porphyry copper deposits. *Nat. Rev. Earth Env.* **2**, 542–557 (2021).
57. Z. Q. Hou, Z. M. Yang, Y. J. Lu, A. Kemp, Y. C. Zheng, Q. Y. Li, J. X. Tang, Z. S. Yang, L. F. Duan, A genetic linkage between subduction- and collision-related porphyry cu deposits in continental collision zones. *Geology* **43**, 247–250 (2015).
58. Y.-C. Zheng, S.-A. Liu, C.-D. Wu, W. L. Griffin, Z.-Q. Li, B. Xu, Z.-M. Yang, Z.-Q. Hou, S. Y. O'Reilly, Cu isotopes reveal initial Cu enrichment in sources of giant porphyry deposits in a collisional setting. *Geology* **47**, 135–138 (2019).
59. R. L. Rudnick, S. R. Taylor, The composition and petrogenesis of the lower crust: A xenolith study. *J. Geophys. Res.* **92**, 13981–14005 (1987).
60. R. L. Rudnick, S. L. Goldstein, The Pb isotopic compositions of lower crustal xenoliths and the evolution of lower crustal Pb. *Earth Planet. Sci. Lett.* **98**, 192–207 (1990).
61. P. D. Kempton, R. S. Harmon, Oxygen isotope evidence for large-scale hybridization of the lower crust during magmatic underplating. *Geochim. Cosmochim. Acta* **56**, 971–986 (1992).
62. A. E. Saal, R. L. Rudnick, G. E. Ravizza, S. R. Hart, Re-Os isotope evidence for the composition, formation and age of the lower continental crust. *Nature* **393**, 58–61 (1998).
63. J. D. Vervoort, P. J. Patchett, F. Albarede, J. Blichert-Toft, R. Rudnick, H. Downes, Hf-Nd isotopic evolution of the lower crust. *Earth Planet. Sci. Lett.* **181**, 115–129 (2000).
64. F.-Z. Teng, R. L. Rudnick, W. F. McDonough, S. Gao, P. B. Tomascak, Y. S. Liu, Lithium isotopic composition and concentration of the deep continental crust. *Chem. Geol.* **255**, 47–59 (2008).
65. Y.-C. Liu, A.-D. Wang, F. Rolfo, C. Groppo, X.-F. Gu, B. Song, Geochronological and petrological constraints on Palaeoproterozoic granulite facies metamorphism in southeastern margin of the North China Craton. *J. Metamorphic Geol.* **27**, 125–138 (2009).
66. Y.-C. Liu, A.-D. Wang, S.-G. Li, F. Rolfo, Y. Li, C. Groppo, X.-F. Gu, Z.-H. Hou, Composition and geochronology of the deep-seated xenoliths from the southeastern margin of the North China Craton. *Gondw. Res.* **23**, 1021–1039 (2013).
67. Z.-Z. Wang, S.-A. Liu, S. Ke, Y.-C. Liu, S.-G. Li, Magnesium isotopic heterogeneity across the cratonic lithosphere in eastern China and its origins. *Earth Planet. Sci. Lett.* **451**, 77–88 (2016).
68. L. Guo, O. E. Jajoutz, W. J. Shinevar, H. Zhang, Formation and composition of the Late Cretaceous Gangdese arc lower crust in southern Tibet. *Contrib. Mineral. Petrol.* **175**, 58 (2020).

69. Z. M. Zhang, H. X. Ding, R. M. Palin, X. Dong, Z. L. Tian, Y. F. Chen, The lower crust of the Gangdese magmatic arc, southern Tibet, implication for the growth of continental crust. *Gondw. Res.* **77**, 136–146 (2020).
70. J. Davidson, S. Turner, H. Handley, C. Macpherson, A. Dosseto, Amphibole "sponge" in arc crust? *Geology* **35**, 787–790 (2007).
71. A. L. Liu, Q. Wang, D. C. Zhu, Z. D. Zhao, S. A. Liu, R. Wang, J. Dai, Y. C. Zheng, L. Zhang, Origin of the ca. 50 Ma Linzizong shoshonitic volcanic rocks in the eastern Gangdese arc, southern Tibet. *Lithos* **304-307**, 374–387 (2018).
72. S.-J. Wang, F.-Z. Teng, S.-G. Li, J.-A. Hong, Magnesium isotopic systematics of mafic rocks during continental subduction. *Geochim. Cosmochim. Acta* **143**, 34–48 (2014).
73. A. I. Okay, S. T. Xu, A. M. C. Sengör, Coesite from the Dabie Shan eclogites, Central China. *Eur. J. Mineral.* **1**, 595–598 (1989).
74. C. N. Maréchal, P. Télouk, F. Albarède, Precise analysis of copper and zinc isotopic compositions by plasma-source mass spectrometry. *Chem. Geol.* **156**, 251–273 (1999).
75. S.-A. Liu, D. D. Li, S. G. Li, F.-Z. Teng, S. Ke, Y. S. He, Y. H. Lu, High-precision copper and iron isotope analysis of igneous rock standards by MC-ICP-MS. *J. Anal. At. Spectrom* **29**, 122–133 (2014).
76. D. J. Miller, R. R. Loucks, M. Ashraf, Platinum-group element mineralization in the Jijal layered ultramafic-mafic complex, Pakistani Himalayas. *Econ. Geol.* **86**, 1093–1102 (1991).
77. B. R. Hacker, P. B. Kelemen, M. D. Behn, Continental lower crust. *Annu. Rev. Earth Planet. Sci.* **43**, 167–205 (2015).
78. Y. Zhao, C. J. Xue, S.-A. Liu, R. Mathur, X. B. Zhao, Y. Q. Yang, J. F. Dai, R. H. Man, X. M. Liu, Redox reactions control Cu and Fe isotope fractionation in a magmatic Ni–Cu mineralization system. *Geochim. Cosmochim. Acta* **249**, 42–58 (2019).
79. Z. Chen, J. Chen, L. S. Tamehe, Y. Zhang, Z. Zeng, X. Xia, Z. Cui, T. Zhang, K. Guo, Heavy copper isotopes in arc-related lavas from cold subduction zones uncover a sub-arc mantle metasomatized by serpentinite-derived sulfate-rich fluids. *J. Geophys. Res. Solid Earth* **127**, e2022JB024910 (2022).
80. S.-A. Liu, "Geochemical studies on petrogenesis of Mesozoic adakitic rocks in central-eastern China and high-temperature magnesium isotope fractionation", PHD thesis, University of Science and Technology of China (2011).
81. W.-R. Liu, Z.-Z. Wang, S.-A. Liu, Zinc isotopic systematics of deep crustal xenoliths from the southeastern North China craton and implications for intra-crustal differentiation. *Lithos* **448-449**, 107178 (2023).
82. S.-A. Liu, T. Wu, S.-G. Li, Z.-Z. Wang, J. Liu, Contrasting fates of subducting carbon related to different oceanic slabs in East Asia. *Geochim. Cosmochim. Acta* **324**, 156–173 (2022).
83. N. Dauphas, M. Roskosz, E. E. Alp, D. R. Neuville, M. Y. Hu, C. K. Sio, F. L. H. Tissot, J. Zhao, L. Tissandier, E. Médard, C. Cordier, Magma redox and structural controls on iron isotope variations in Earth's mantle and crust. *Earth Planet. Sci. Lett.* **398**, 127–140 (2014).
84. Y. Li, A. Audétat, Partitioning of V, Mn, Co, Ni, Cu, Zn, As, Mo, Ag, Sn, Sb, W, Au, Pb, and Bi between sulfide phases and hydrous basanite melt at upper mantle conditions. *Earth Planet. Sci. Lett.* **355-356**, 327–340 (2012).

Acknowledgments: We are grateful to the editor, G. Gaetani, for efficient editorial handing and to M. Chiaradia, E. J. Chin, and J.-W. Park for constructive comments and suggestions that improved the manuscript. We thank Y.-C. Zheng for providing cumulate samples from the Gangdese arc, D.-C. Zhu for providing the basalt and basaltic andesite samples from Tibet, S.-J. Wang for providing the metamorphosed rock samples, and K.-X. Song and Y.-R. Qu for help in the laboratory. **Funding:** This work is supported by the National Natural Science Foundation of China (grant no. 42121002) and the National Key R&D Program of China (2019YFA0708400) to S.-A.L. **Author contributions:** S.-A.L. designed the study, collected lower crustal samples from Xuzhou-Bengbu, and performed Cu isotopic analyses. R.L.R. collected and characterized lower crustal xenoliths from North Queensland, Australia. W.-R.L. participated in sample collection and performed elemental and TIMA analysis. T.-H.W. collected reference data. All authors contributed extensively to the interpretation of the data, discussions, and preparation of the manuscript. **Competing interests:** The authors declare that they have no competing interests. **Data and materials availability:** All data needed to evaluate the conclusions in the paper are present in the paper and/or the Supplementary Materials.

Submitted 15 January 2023
Accepted 4 August 2023
Published 6 September 2023
10.1126/sciadv.adg6995